OPTOELECTRONICS AND ADVANCED MATERIALS – RAPID COMMUNICATIONS Vol. 4, No. 5, May 2010, p. 754 - 758

Remote and in-situ seawater bio-optical description during the XVIII oceanographic expedition

R. FANTONI, L. FIORANI[a*], S. LORETI[b], A. PALUCCI[a], L. LAZZARA[c], I. NARDELLO[d]
ENEA, UTAPRAD, Via Fermi 45, 00044 Frascati, Italy
[a]ENEA, UTAPRAD-DIM, Via Fermi 45, 00044 Frascati, Italy
[b]ENEA, METR, Via Anguillarese 301, 00123 Roma, Italy
[c]University of Florence, Department of Evolutionistic Biology "Leo Pardi", Via Romana 17-19, 50125 Florence, Italy
[d]National University of Ireland, Institute for Environment, Marine and Energy, University Road, Galway, Ireland

During the XVIII oceanographic expedition of the Italian Antarctic Research Program, the bio-optical properties of seawater have been characterized by in-situ and remote sensors. In particular, the absorption and fluorescence of chromophoric dissolved organic matter (CDOM) have been measured by the absorption and attenuation meter WET Labs AC-9-25 and by the ENEA lidar fluorosensor, respectively. The data of those instruments have been used to develop a CDOM bio-optical algorithm for the Sea-viewing Wide Field-of-view Sensor (SeaWiFS). Such algorithm has been applied to the Ross Sea sector of the Southern Ocean and its results have been compared with the CDOM values obtained by other authors. Moreover, CDOM and chlorophyll-a maps have been released in order to reveal the relationships in the spatio-temporal dynamics of these two biomass indicators.

(Received 06, May 2010; accepted May 20, 2010)

Keywords: Chlorophylls, Dissolved organic matter, Absorption spectroscopy, Lidar, Radiometers, Algorithms

1. Introduction

The Southern Ocean (SO) is still one of the less known regions of the world because of its large extent, relative inaccessibility and high variability. In particular, the bio-optical properties of the SO have been poorly described. Nevertheless, this knowledge is essential for ecological studies of the pelagic system, especially when ocean color remote sensing is used to describe that oceanic province.

Organic carbon in the world oceans is present mainly as dissolved organic matter (DOM) and large part of it is chromophoric DOM (CDOM) [Kirkpatrick et al. 2003]: therefore, investigating the distribution and dynamics of CDOM will help us to understand the global carbon cycle. In addition, CDOM is directly linked to phytoplankton at least in two ways. From one hand, CDOM limits light penetration in seawater and, as a consequence, regulates algal growth [Olaizola et al. 1986]. From the other one, phytoplankton exudation and degradation in algal blooms can increase CDOM concentration. A third reason to study CDOM is that it is correlated with dymethil sulfide (DMS), a climate-driving factor, through a feedback process controlled by phytoplankton [Toole and Siegel 2004], which can not be directly measured by present ocean color satellite radiometers.

Unfortunately, CDOM is not among the data products usually provided by satellite radiometers: e.g. a standard CDOM algorithm is not available for the Sea-viewing Wide Field-of-view Sensor (SeaWiFS) [Hooker et al. 1992], even if the SeaWiFS Project Office recognized its usefulness [McClain et al. 2004]. Nevertheless, some algorithms have been suggested for the calculation of the CDOM absorption coefficient from ocean color data products [Aiken et al. 1995, Hoge et al. 1999, Johannessen et al. 2003, Siegel et al. 2002].

To sum up, CDOM is a key oceanic variable and the debate on its satellite retrieval is still open: this explain the research effort in calibrating a CDOM algorithm for water-leaving radiance data, collected by space borne radiometers. Such algorithm has been developed thanks to the measurements carried out by the ENEA Lidar Fluorosensor (ELF) [Barbini et al. 2001] onboard the research vessel Italica, during the XVIII oceanographic expedition of the Italian Antarctic Research Program, performed from 5 January to 4 March 2003 in the Ross Sea, with particular emphasis on coastal zones and polynya areas. ELF is based on laser-induced fluorescence (LIF) and continuously provides concentrations of CDOM and phytoplankton pigments all along the ship track. The approach of this study is similar to that followed for a lidar calibrated chlorophyll-a (Chl-a) algorithm [Barbini et al. 2003] and requires the retrieval of the CDOM absorption coefficient from fluorescence measurements [Hoge et al. 1995]. In other words, a regional CDOM bio-optical algorithm merging in-situ and remote sensing has been developed: starting from in-situ absorption and LIF, satellite radiance is converted into CDOM absorption and the corresponding imagery is released and compared with the biomass distribution. Those results are useful to understand the marine biodynamics, e.g. the relation between Chl-a and CDOM and have been applied here in the Ross Sea Region (RSR), i.e. the area delimited by the coast and a line (straight in the cylindrical equidistant

projection) from a point near Cape Adare (72° S, 170° E) to a point near Cape Colbeck (76° S, 158° W), and the Ross Sea Sector (RSS) defined as the zone of SO from the coast of Antarctica north to 50° S latitude in the 160° E – 130° W interval.

2. Methods

2.1 In-situ measurements

During the XVIII oceanographic expedition, the water column was sampled at discrete depths of the photic zone with Niskin-type bottles, in 25 stations of the western Ross Sea (Fig. 1). Filtration (Whatmann GF/F) of up to 3 liters of seawater provided assessment of the concentration of the photosynthetic lipophylic pigments (HPLC analysis) and of organic C and N composition of the particulate matter (CHN elemental analyzer, PE). Filters were also collected to analyze the spectral variation of the absorption coefficient of total particulate matter, detritus and phytoplankton. Spectral measurements of the inherent and apparent optical properties were performed through the absorption and attenuation meter WET Labs AC-9-25 [Van Zee and Walsh 2004] and the spectral radiometer Satlantic OCI-200 in 19 stations of the western Ross Sea.

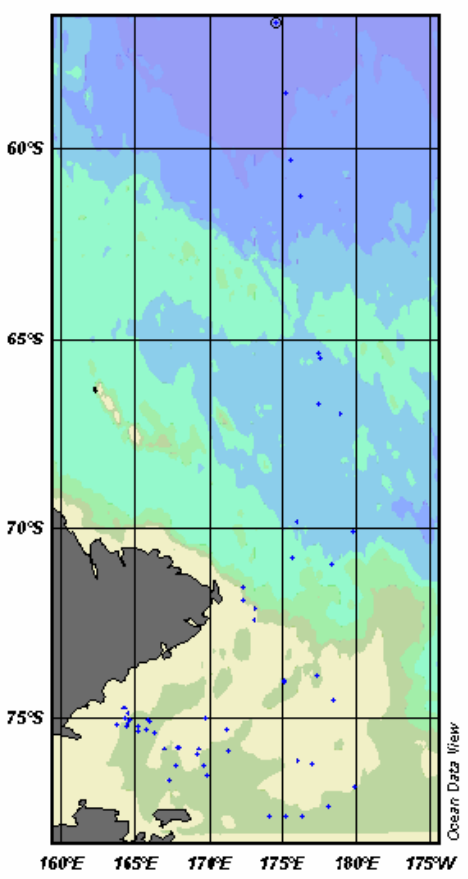

Fig. 1. AC-9-25 stations sampled during the XVIII oceanographic expedition.

AC-9-25 determines spectral transmittance and spectral absorption of natural and filtered seawater over nine wavelengths: 412, 440, 488, 510, 555, 630, 650, 676 and 715 nm (due to an instrument problem, absorption has not been measured at 715 nm during the campaign). At 412 and 440 nm, the total absorption of filtered seawater corresponds to a_{CDOM} because other effects are negligible for $\lambda < 500$ nm [Aiken et al. 1995]. The variability of the crossed seawaters is clearly shown in the absorption spectra measured and reported in Fig. **Error! Bookmark not defined.**, in case of natural seawater.

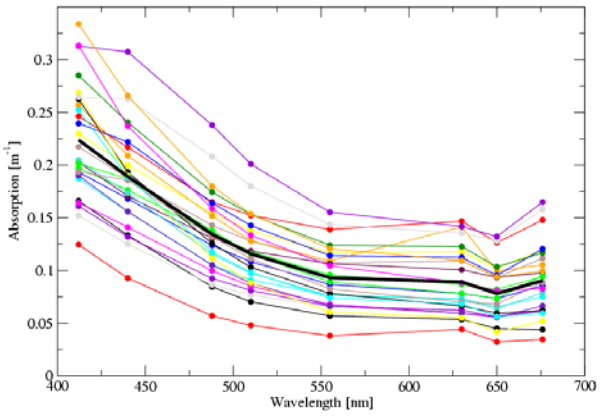

Fig. 2. AC-9-25 measurements of absorption of natural seawater (a_w) carried out in 26 stations along the lidar track for 8 spectral channels (bold black line: average values).

2.2 SeaWiFS calibration

Details and references on SeaWiFS, ELF and Chl-a algorithms can be found in Hooker et al. [1992] and Barbini et al. [2003], here we focus on the ELF-calibration of the CDOM algorithm. The ELF optical channels at 404 and 450 nm correspond to Raman scattering of water and fluorescence of CDOM, respectively. The CDOM fluorescence signal (f_{CDOM}) is released in Raman units (RU), i.e. it is normalized to the water Raman peak [Barbini et al. 2001]. Afterwards, it is converted into CDOM absorption (a_{CDOM}) through calibration with the measurements carried out with AC-9-25: ELF and AC-9-25 operated simultaneously in several stations of the oceanographic campaign. The best correlation between f_{CDOM} and a_{CDOM} has been found at 440 nm: this explains why a_{CDOM} at 440 nm has been used to calibrate f_{CDOM}. The final results of the ELF calibration are given in Table 1. The details of the statistical treatment can be found elsewhere [Fantoni et al. 2005].

Table 1. Results of the calibration of ELF by AC-9-25 (a_1 is the slope, σ_1 is the slope error and R is the correlation coefficient).

# of points	a_1 [m^{-1} RU^{-1}]	σ_1 [m^{-1} RU^{-1}]	R
35	0.052	0.003	0.74

ELF CDOM data, now expressed in m^{-1}, can be used for the ELF-calibration of the SeaWiFS CDOM algorithm, exactly in the same way ELF Chl-a data has been used for the ELF calibration of the SeaWiFS Chl-a algorithm, as described in Barbini et al. [2003]. The only difference is that normalized water leaving radiance (Lwn) at 443 and 510 nm is employed, instead of that at 490 and 555 nm. The rationale of choosing those wavelengths is that a_{CDOM} is strong at 443 nm (on channel) and weak at wavelengths greater than 500 nm (off channel) [Aiken et al. 1995]. The use of Lwn(412 nm) has been avoided because of problems with atmospheric correction at short wavelengths [Siegel et al. 2000]. The 510-nm channel has been preferred to the 555-nm channel because it is less affected by suspended inorganic material [Hooker et al. 1992] and for its relative proximity to the 531-nm channel of the Moderate Resolution Imaging Spectroradiometer (MODIS) [Esaias et al. 1998], in view of an extension of this study to that sensor. The parameters of the linear fit calibrating SeaWiFS are given in Table 2. Once more, the details of the statistical treatment can be found in Fantoni et al. [2005]: here we observe only that the lidar a_{CDOM} data are fitted on the SeaWiFS band ratios Lwn(443)/Lwn(510) in a log-log plot, thus providing an algorithm for the retrieval of CDOM from radiance, as in common Chl-a bio-optical algorithms.

Table 2. Results of the calibration of SeaWiFS by ELF (a_0 is the intercept, σ_0 is the intercept error, a_1 is the slope, σ_1 is the slope error and R is the correlation coefficient).

# of points	a_0 [$\log_{10}$ m^{-1}]	σ_0 [$\log_{10}$ m^{-1}]	a_1 [$\log_{10}$ m^{-1}]	σ_1 [$\log_{10}$ m^{-1}]	R
899	-1.012	0.007	-1.39	0.05	0.69

In principle, one could calibrate SeaWiFS directly by AC-9-25 but, in practice, the procedure followed here has two advantages:

1. ELF data are more suitable to that purpose than AC-9-25 samplings because their geographic coverage and spatial resolution are closer to image extent and pixel size, respectively, of the SeaWiFS data products,
2. the number of ELF measurements is much larger than that of AC-9-25 stations.

3. Results

The ELF-calibration of the SeaWiFS algorithm for CDOM has been carried out in RSR. Nevertheless, the ELF-calibrated SeaWiFS algorithms for CDOM and Chl-a were applied also to a wider zone, RSS. Spatially averaged CDOM values in RSR and RSS obtained during the XVIII oceanographic expedition with level 3 (L3) 8-day standard mapped image (SMI) products are shown in Fig. 3. The average values for the whole campaign are ~ 0.075 m^{-1} in RSR and ~ 0.055 m^{-1} in RSS. It is not surprising that CDOM values were higher in the costal zone than in the open ocean: CDOM is often a degradation product of phytoplankton and phytoplankton concentration is usually higher in the coastal zone. This is confirmed by the CDOM peak in RSR of Fig. 3, nearly simultaneous to an algal bloom.

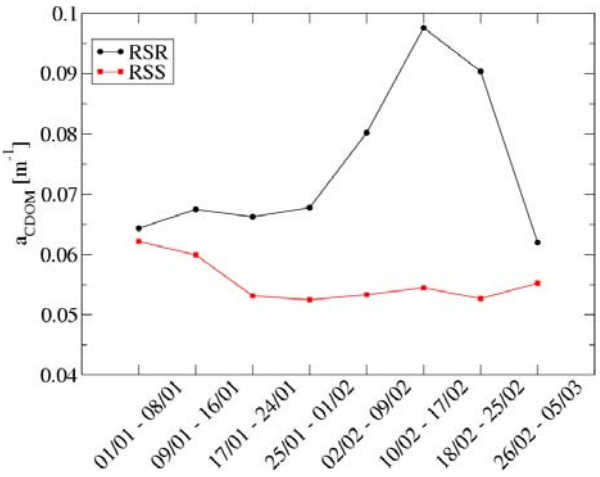

Fig. 3. Spatial averages in RSR and RSS of ELF-calibrated SeaWiFS-retrieved a_{CDOM} during the XVIII oceanographic expedition.

Examples of Chl-a and CDOM distribution maps, retrieved with L3 8-day SMI products, are shown in Fig. 4 (a) and (b), respectively, where the continuous line represents the ship track. Missing satellite pixels are due to sea ice or to the cloud coverage on free waters. According to the observation in the visible band and in the microwave region by the National Oceanic and Atmospheric Administration (NOAA) satellites OLS and SSM/I, respectively, the cloud coverage is the main obstacle to SeaWiFS imaging of the ocean at high latitudes, while sea ice dominates at low latitudes. Austral summer 2002-2003 has been characterized by an exceptionally large ice coverage. This explains why only few satellite pixels have been acquired in the Ross Sea from the half of February. On the contrary, it can be pointed out that ELF is not sensitive at all to clouds and it carries out measurements also in polynyas. Fig. 4 shows that phytoplankton blooms develop in ice free regions (near Terra Nova Bay and Ross Island) and in the Antarctic Divergence, an upwelling zone where nutrients are released. Once more, Chl-a and CDOM correlate, suggesting that CDOM arises mainly from phytoplankton degradation, at least in the region and the period under study.

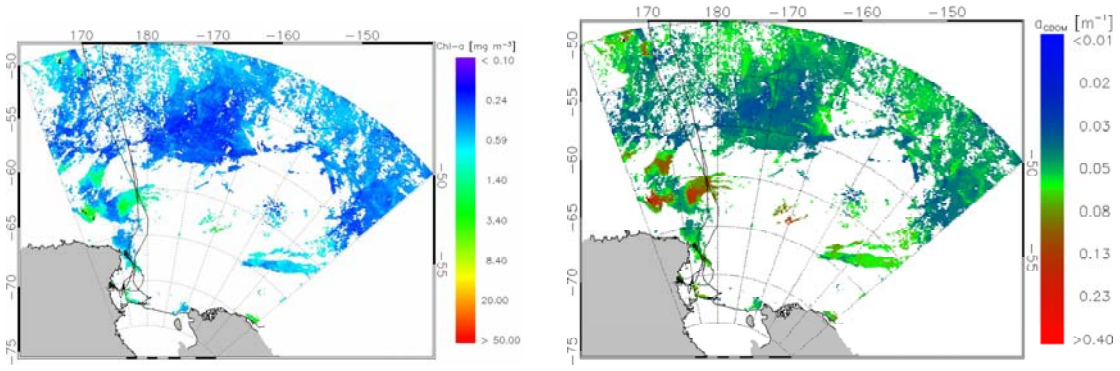

(a) *(b)*

Fig. 4. Temporal averages in the period from 17 to 24 January 2003 of ELF-calibrated SeaWiFS-retrieved Chl-a (a) and a_{CDOM} (b) in RSS.

In general, the values of a_{CDOM} found in this study compare quite well with literature data of the Ross Sea. In particular they are:

- higher than the measurements taken in a former oceanographic campaign carried out in 1997 [Mitchell 2003] and reported in Table 3,
- similar to the values of a semi-analytical algorithm applied to 1998 [Siegel et al. 2000] (about 0.1 m^{-1});
- comparable to the results of an empirical algorithm relative to a 7-year period (1997 – 2004) [Fichot and Miller 2004] (around 0.2 m^{-1}).

Table 3. a_{CDOM} measured during the AESOPS (at 442 nm) and the XVIII (at 440 nm) oceanographic expeditions.

Oceanographic campaign	Mean	Standard Deviation	Max	Min	# of stations	Period	Zone
AESOPS	0.027	0.021	0.140	0.001	40	09/11/97 – 14/03/98	53° S – 77° S 169° E – 166° W
XVIII	0.075	0.033	0.176	0.047	26	05/01/03 – 05/03/03	53° S – 78° S 164° E – 177° W

4. Conclusions

The variability of the biological and optical properties of the Ross Sea has been investigated by merging active (laser) and passive (satellite) remote sensing data. In particular, an original ELF-calibrated SeaWiFS algorithm for CDOM has been developed in the Ross Sea with the measurements of the XVIII oceanographic expedition (Austral summer 2002-2003).

The application of that algorithm to L3 8-day SMI SeaWiFS products in the SO provided new estimates of a_{CDOM} at 440 nm. The results of this study compare well with literature data, especially with recent values, higher than those found in previous works.

The comparison between simultaneous ELF-calibrated SeaWiFS Chl-a and CDOM images improve our knowledge on spatial distributions and temporal dynamics of both parameters and on the link between phytoplankton and DOM.

Acknowledgements

This work has been supported by PRNA–Oceanographic Sector–8.3 Project "ARES–active and passive remote sensing of the Southern Ocean for the monitoring of the biological parameters". The important contribution of F. Colao is kindly acknowledged. The authors would like to thank the SeaWiFS Project (Code 970.2) and the Distributed Active Archive Center (Code 902) at the Goddard Space Flight Center, Greenbelt, MD 20771, for the production and distribution of these data, respectively. These activities are sponsored by NASA's Mission to Planet Earth Program.

References

[1] J. Aiken, G. F. Moore, C. C. Trees, S. B. Hooker, D. K. Clark, In: Hooker, S. B. and Firestone, E. R. (Eds.), SeaWiFS Technical Report Series. NASA, Greenbelt, US, **29**, 1995.

[2] R. Barbini, F. Colao, R. Fantoni, L. Fiorani, A. Palucci, J. Optoelectron. Adv. Mater. **3**(4), 817 (2001).

[3] R. Barbini, F. Colao, R. Fantoni, L. Fiorani, A. Palucci, International Journal of Remote Sensing **24**, 3205 (2003).

[4] W. E. Esaias, M. R. Abbott, I. Barton, O. B. Brown, J. W. Campbell, K. L. Carder, D. K. Clark, R. H. Evans, F. E. Hoge, H. R. Gordon, W. M. Balch, R. Letelier, P. J. Minnett, IEEE Transactions on Geoscience and Remote Sensing **36**, 1250 (1998).

[5] R. Fantoni, L. Fiorani, A. Palucci, I. G. Okladnikov, New algorithm for CDOM retrieval from satellite imagery, ENEA, Rome, Italy, 2005.

[6] C. G. Fichot, W. L. Miller, E-proceedings of Ocean Optics XVII. ONR, Fremantle, Australia, CD-ROM, 2007.

[7] F. E. Hoge, A. Vodacek, R. N. Swift, J. K. Yungel, N. V. Blough, Applied Optics **34**, 7032 (1995).

[8] F. E. Hoge, C. W. Wright, P. E. Lyon, R. N. Swift, J. K. Yungel, Applied Optics **38**, 495 (1999).

[9] S. B. Hooker, W. E. Esaias, G. C. Feldman, W. W. Gregg, C. R. McClain, In: Hooker, S. B. and Firestone, E. R. (Eds.), SeaWiFS Technical Report Series. NASA, Greenbelt, US, **1**, 1992.

[10] S. C. Johannessen, W. L. Miller, J. J. Cullen, Journal of Geophysical Research **108**(C9), 3301 (2003).

[11] G. J. Kirkpatrick, C. Orrico, M. A. Moline, M. Oliver, O. M. Schofield, O. M., Applied Optics **42**, 6564 (2003).

[12] C. R. McClain, G. C. Feldman, S. B. Hooker, Deep-Sea Research **II51**, 5 (2004).

[13] G. Mitchell, In: US JGOFS Data Management Office (Ed.), US JGOFS Process Study Data 1989-1998. WHOI, Woods Hole, US, **1**, Version 1, CD-ROM, 2003.

[14] M. Olaizola, R. J. Geider, W. G. Harrison, L. M. Graziano, G. M. Ferrari, P. M. Schlittenhardt, Limnology and Oceanography **41**, 755 (1986).

[15] D. A. Siegel, S. Maritorena, N. B. Nelson, D. A. Hansell, M. Lorenzi-Kayser, Journal of Geophysical Research, **107**(C12), 3228 (2002).

[16] D. A. Siegel, M. Wang, S. Maritorena, W. Robinson, Applied Optics **39**, 3582 (2000).

[17] D. A. Toole, D. A. Siegel, Geophysical Research Letters **31,** L09308 (2004).

[18] H. Van Zee, I. Walsh, I., WET Labs, Philomath, US, 2004.

*Corresponding author: luca.fiorani@enea.it